

Anti-solar differential rotation and surface flow pattern on UZ Libræ

K. Vida^{1,2,*}, Zs. Kővári², M. Švanda^{3,4}, K. Oláh², K. G. Strassmeier⁵, J. Bartus⁵, and E. Forgács-Dajka¹

¹ Eötvös University, Department of Astronomy, H-1518 Budapest, P.O.Box. 32, Hungary

² Konkoly Observatory, H-1525 Budapest, P.O.Box 67, Hungary

³ Astronomical Institute, Academy of Sciences of the Czech Republic, v. v. i., Fričova 298, 251 65 Ondřejov, Czech Republic

⁴ Astronomical Institute, Faculty of Mathematics and Physics, Charles University in Prague, V Holešovičkách 2, 180 00 Prague 8, Czech Republic

⁵ Astrophysical Institute Potsdam, An der Sternwarte 16, D-14482 Potsdam, Germany

Received xx xxx 2007, accepted xx xxx 2007

Published online later

Key words stars: activity – stars: spots – stars: imaging

We re-investigate UZ Libræ spectra obtained at KPNO in 1998 and 2000. From the 1998 data we compose 11 consecutive Doppler images using the Ca I-6439, Fe I-6393 and Fe I-6411 lines. Applying the method of average cross-correlation of contiguous Doppler images we find anti-solar differential rotation with a surface shear of $\alpha \approx -0.03$. The pilot application of the local correlation tracking technique for the same data qualitatively confirms this result and indicates complex flow pattern on the stellar surface. From the cross-correlation of the two available Doppler images in 2000 we also get anti-solar differential rotation but with a much weaker shear of $\alpha \approx -0.004$.

© 2007 WILEY-VCH Verlag GmbH & Co. KGaA, Weinheim

1 Introduction

In our time, the Sun is the only star for which the surface differential rotation and other surface flows can be measured directly. The detection of differential rotation on active stars, however, is a challenging observational task. Starspots are regarded as manifestations of solar-like active regions and as such, are suitable for tracking and recovering surface flows. In this paper we make one of the first attempts at recovering surface flows on spotted stars (see also the paper by Kővári et al. 2007a).

Our target is the RSCVn-type active giant star UZ Libræ. The star has a very fast rotation rate of $P_{\text{rot}} = 4.76$ days, which is equivalent to the orbital period. Doppler images of the star were presented by Strassmeier (1996) and Oláh, Strassmeier & Weber (2002). In the latter paper the signature of a weak anti-solar differential rotation (DR) was found but the authors regarded the detection inconclusive. The possible DR was also examined by Oláh Jurcsik and Strassmeier (2003) using photometric observations. They found two permanent, distinct periods in the Fourier-spectrum of the long-term data, which were assigned to the different rotation rate of spots at high and low latitudes, resulting in $\alpha = \Delta\Omega/\Omega$ of -0.0026 . Adopted stellar parameters of UZ Lib are summarised in Table 1, the values which are not marked were taken from Oláh, Strassmeier & Weber (2002).

Table 1 Stellar parameters of UZ Libræ

spectral type ¹	K0 III
$P_{\text{rot}} = P_{\text{orb}}$ ^{2,3}	4.768241 days
$v \sin i$ ^{2,3}	$67 \pm 1 \text{ km s}^{-1}$
i ⁴	$50^\circ \pm 10^\circ$
T_{eff} ³	4800 K
$\log g$ ²	2.5
Microturbulence ξ	0.8 km s^{-1}
Macroturbulence $\zeta_R = \zeta_T$	4 km s^{-1}
Chemical abundance	solar

¹ Bopp & Stencel (1981)

² Strassmeier (1996)

³ Fekel et al. (1999)

2 Data processing

We used two sets of spectra obtained at Kitt Peak National Observatory (KPNO) in 1998 and 2000. From the 16 spectra obtained in 1998 we recover a time-series of 11 Doppler images. For the first image we take the first six spectra, and run our inversion code TEMP MAP (Rice et al. 1989) for the Ca I-6439, Fe I-6393 and Fe I-6411 mapping lines. Then, we proceed with the next set of six spectra, leaving the first spectrum and adding the subsequent one (i.e., the 7th) to the modelled dataset, producing a slightly different Doppler image. This pattern is followed until we get the last image from the last six spectra of the time-series. The respective Doppler images for the three different mapping lines are in quite good agreement with each other and are averaged for

* Corresponding author: e-mail: k.vida@elte.hu

further use, resulting in a time-series of 11 Doppler images covering about 20 days (4.2 rotation cycles). Note, that a similar method was applied to get a motion picture of the surface spots on HR 1099 (Strassmeier & Bartus 2000) and later on LQ Hya (Kővári et al. 2004). From the 17 spectra gathered in 2000 we reconstructed only two images from two subsets consisting of 8 and 9 spectra, both covering about 8 days, but separated by a time lag of 16 days (Oláh, Strassmeier & Weber 2002).

3 Results from the cross-correlation study

The method of ‘Average Cross-CORrelation of contiguous Doppler images’ (hereafter ACCORD) uses a combination of independent image pairs (i.e., which do not have common spectra), whose relevant latitude strips are cross-correlated with each other. When having multiple cross-correlation maps, the elapsed time lags between the correlated images are different, so in order to average them, one has to normalize the cross-correlation maps (i.e., applying a linear stretching or compression along the longitude shift) depending on the time lag. Unfortunately, the larger the time lag between the cross-correlated images, the greater the risks of masking the DR pattern by individual spot evolutions (waxing or waning of spots, emerging of new spots, melting, etc.). Thus, to minimize this effect, we correlate only the consecutive but contiguous (i.e., the closest independent) images. The average cross-correlation map is then fitted by a quadratic differential rotation law: $\Omega(\vartheta) = \Omega_{\text{eq}} - \Delta\Omega \sin^2 \vartheta$, where ϑ stands for latitude, Ω_{eq} means the angular velocity on the equator, and $\Delta\Omega = \Omega_{\text{eq}} - \Omega_{\text{pole}}$ the angular velocity difference between the equator and the poles. The differential rotation parameter is derived as $\alpha = \Delta\Omega/\Omega_{\text{eq}}$. For a detailed description of this method, as well as for further applications see Kővári et al. (2004, 2007b).

The resulting cross-correlation maps are plotted in Fig. 1 for 1998 (top) and for 2000 (bottom). The best correlated longitude shifts are fitted by a quadratic DR law. The best-fit rotation function indicates zero longitude shift of the equatorial zone, i.e., the equator is rotating with the orbital period. This result agrees well with the findings in Oláh, Jurcsik & Strassmeier (2003). The derived α parameters are -0.027 ± 0.003 and -0.004 ± 0.001 for the 1998 and 2000 data, respectively, indicating a weak anti-solar differential rotation in both cases, matching (at least qualitatively) the negative DR parameter derived from photometric data by Oláh, Jurcsik & Strassmeier (2003).

The cross-correlation study can be repeated for the corresponding longitudinal stripes (meridian circles). This case we take only the hemisphere of the always visible pole, because Doppler imaging is more reliable for this part. We then look for the correlation pattern in the same way when searching for DR from longitudinal cross-correlation. The resulting latitudinal cross-correlation pattern is shown in

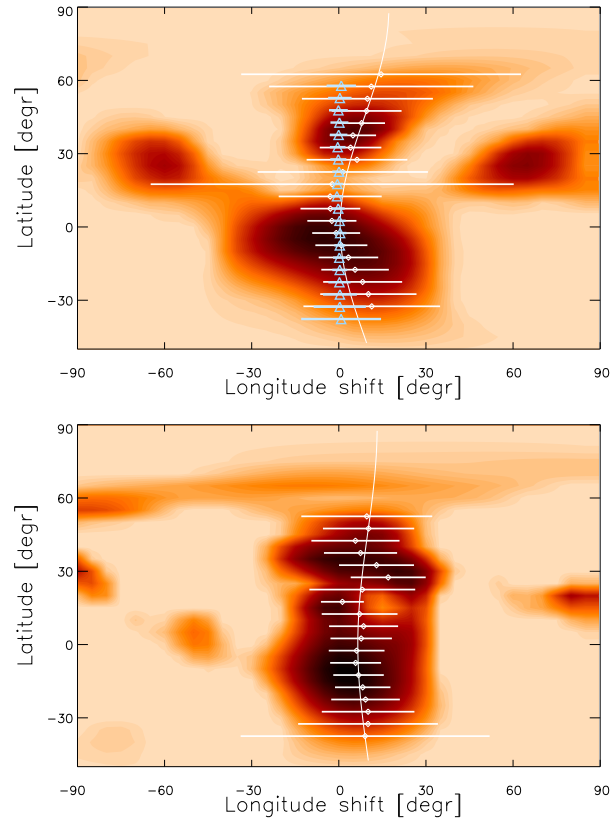


Fig. 1 Cross-correlation maps obtained from 11 time-series Doppler images in 1998 (top) and from 2 Doppler images in 2000 (bottom). The better the correlation the darker the shade. Cross-correlation functions per latitude are fitted by Gaussian curves (Gaussian peaks are indicated by dots, the FWHMs by error bars). The continuous line shows the fitted quadratic differential rotation law. Longitude shifts from the LCT method are overplotted as triangles in the top panel (see Sect. 4 for details).

Fig. 3 (top). The best correlated latitude shifts indicate incoherent flows, with too large error bars.

4 Results from local correlation tracking

We also apply the local correlation tracking (hereafter LCT) technique, which was originally designed to remove seeing-induced distortion in sequences of solar images. This technique examines the best match between the pixels of the consecutive images in a correlation window. The best match defines a vector of displacement, which, as a result gives a map of surface flow patterns. For further details of the method as well as for application see Švanda et al. (2006, 2007) and our forthcoming paper for numerical tests on artificial data by Švanda et al. (2008).

The resulting surface flow map for the 1998 data is plotted in Fig. 2, indicating a complex flow pattern with convergent and also divergent flows, and maybe vortex-like features around the spots near 100° . The differential rotation

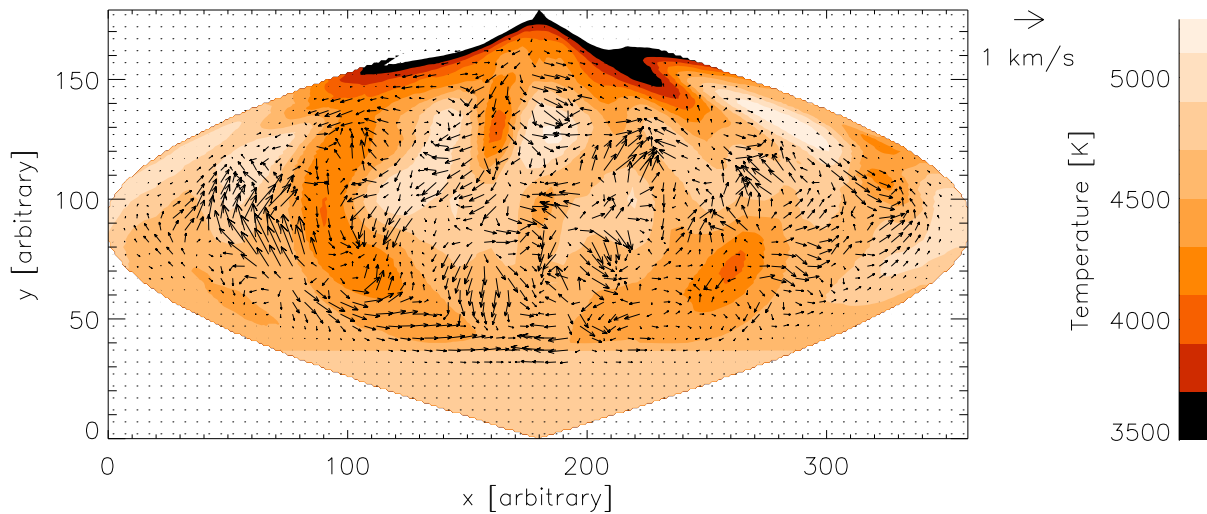


Fig. 2 The result of the LCT technique showing the surface flow pattern on UZ Libræ from the time-series Doppler images in 1998. As a background the average surface temperature map is plotted.

pattern can be derived from averaging the zonal flow components. The best-fit numerical result suggests a weak but uncertain anti-solar shear of -0.001 ± 0.003 which is at least not in a contradiction with the ACCORD results. The latitude shift – longitude diagram from LCT is overplotted on the corresponding ccf-map in Fig. 1 with triangles. Unfortunately, the LCT technique cannot be applied for the two separated subsets in 2000.

From averaging the meridional flow components we are able to investigate the meridional motions. The resulting plot is seen in Fig. 3 (bottom). We get small velocity values in the order of a few hundreds m s^{-1} , and the comparison with the ACCORD result is meaningless.

5 Summary

- Applying our cross-correlation technique ACCORD for the time-series Doppler images of UZLib in 1998 and in 2000 we derived weak surface DR of anti-solar type, in agreement with former DR detections. However, no sign of coherent meridional flow was found.
- LCT technique is applied first time for stellar data (see also the paper by Kővári et al. 2007a) and delineated a complex surface flow network for UZLib.
- Averaging the zonal components of the LCT flow map along latitude resulted in an uncertain, weak anti-solar DR. Meridional flow components show no evidence for any coherent pattern, similarly to the ACCORD non-detection.

Acknowledgements. KV appreciates the hospitality of Konkoly Observatory. KV, ZsK, and KO are grateful to the Hungarian Science Research Program (OTKA) for support under the grant T-048961. ZsK is a grantee of the Bolyai János Scholarship of the Hungarian Academy of Sciences. MŠ is grateful for support by

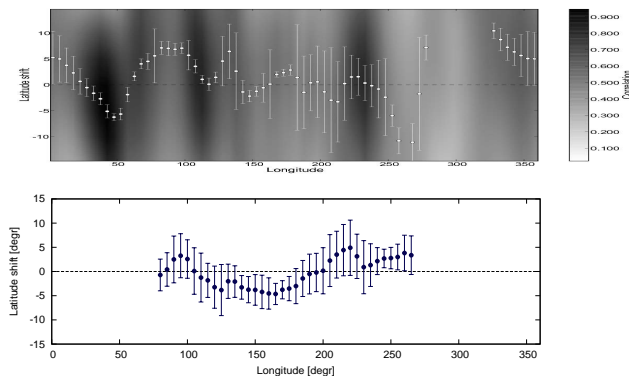


Fig. 3 Best correlated latitudinal shifts from ACCORD (top) and meridional flow components from LCT (bottom). No sign of coherent meridional flow can be seen.

Research Program MSM0021620860 of the Ministry of Education of the Czech Republic.

References

- Bopp, B. W., Stencel, R. E.: 1981, *ApJ* 247, L131
 Fekel, F. C., Strassmeier, K. G., Weber, M., Washuettl, A.: 1999, *A&AS* 137, 369
 Kővári, Zs., Weber, M.: 2004, *PADEU* Vol 14, 221
 Kővári, Zs., Strassmeier, K. G., Granzer, T., Weber, M., Oláh, K., Rice, J. B.: 2004, *A&A* 417, 1047
 Kővári, Zs., Bartus, J., Strassmeier, K. G., Vida, K., Švanda, M., Oláh, K.: 2007a, *AN*, this volume
 Kővári, Zs., Bartus, J., Strassmeier, K. G., Vida, K., Švanda, M., Oláh, K.: 2007b, *A&A* 474, 165
 Oláh, K., Strassmeier, K. G., Weber, M.: 2002, *A&A* 389, 202
 Oláh, K., Jurcsik, J., Strassmeier, K. G.: 2003, *A&A* 410, 685
 Rice, J. B., Wehlau, W. H., Khokhlova, V. L.: 1989, *A&A* 208, 179
 Strassmeier, K. G.: 1996, *A&A* 314, 558

- Strassmeier, K. G., Bartus, J.: 2000, *A&A* 354, 537
Švanda, M., Klvaňa, M., Sobotka, M.: 2006, *A&A* 458, 301
Švanda, M., Zhao, J., Kosovichev, A. G.: 2007, *Sol. Phys.* 241, 27
Švanda, M., Kővári, Zs., Strassmeier, K. G.: 2008, *A&A*, in prep.